

## Generalized Chan-Vese Model for Image Segmentation with Multiple Regions

Dang Tran Vu<sup>1</sup>, Tran Thi Thu Ha<sup>1</sup>, Min Gyu Song<sup>1</sup>, Jin Young Kim<sup>1</sup>, Seung Ho Choi<sup>2</sup>, Asmatullah Chaudhry<sup>1,3</sup>

<sup>1</sup>School of Electronics & Computer Engineering, Chonnam National University, 300 Yongbong Dong, Buk-gu, Gwangju, 500 757, South Korea

<sup>2</sup>Department of Computer Science, Donshin University, Information Center, Kunjae-ro Naju, Chonnam, 520 714, South Korea

<sup>3</sup>HRD, PINSTECH, P.O. Nilore, Islamabad, Pakistan

[syna@jnu.ac.kr](mailto:syna@jnu.ac.kr), [beyondi@jnu.ac.kr](mailto:beyondi@jnu.ac.kr), [0711005.hcmus@gmail.com](mailto:0711005.hcmus@gmail.com), [shchoi@dsu.ac.kr](mailto:shchoi@dsu.ac.kr), [asmat@jnu.ac.kr](mailto:asmat@jnu.ac.kr)

**Abstract:** In this paper, we propose a modified region-based active contour model by integrating the local information of foreground region into Chan-Vese model. Considering local spatial information term in the conventional energy function, our proposed model is able to overcome two limitations of the previous region-based level set methods: a) high sensitivity to the location of initial contours, 2) inability to segment multiple objects. Experimental results show the effectiveness of our proposed method as compared with other major level set-based techniques in terms of both efficiency and accuracy for 2D image segmentation.

[Vu DT, Ha TTT, Song MG, Kim JY, Choi SH, Chaudhry A. **Generalized Chan-Vese Model for Image Segmentation with Multiple Regions.** *Life Sci J* 2013;10(1):1889-1895] (ISSN:1097-8135). <http://www.lifesciencesite.com>. 272

**Keywords:** Generalized Chan-Vese model, region-based active contour, level set method, image segmentation, local information

### 1. Introduction

Deformable models, referred by various names such as snakes, active contours or surfaces, balloons, and deformable contours or surfaces, are one of the most active and successful approaches in image segmentation. The basic idea of deformable models is that modeling curves or surfaces are adjusted for balancing them between internal and external forces (Kass et al., 1987), (Black and Yuille, 1993). Generally, the deformable models can be classified into two categories: parametric deformable models (Amini et al., 1990), (Cohen, 1991), (McInerney et al., 1995) and geometric or level set-based deformable models (Caselles et al., 1993), (Malladi et al., 1995), (Caselles et al., 1997), (Whitaker, 1994). The parametric deformable models represent curves and surfaces explicitly in their parametric forms during deformation. This representation allows direct interaction with the model and leads to a compact representation for real-time implementation. However, adaptation of the model topology, such as splitting or merging parts during the deformation, is not easy using parametric models. On the other hand, geometric deformable models can handle topological changes naturally. These models are based on the theory of curve evolution (Sapiro and Tannenbaum, 1993), (Kimia et al., 1995), (Kimmel et al., 1995), (Alvarez et al., 1993) and the level set method (Osher and Sethian, 1988), (Sethian, 1999) which represent curves and surfaces implicitly as a level set of higher-dimensional scalar function. Such

methodologies are best suited for the recovery of objects with unknown topologies. As a novel approach, geometric deformable models avoid the evolution process of tracing the curve after expressing closed planar curves and 3D closed surfaces. Thus problem of curve evolution is converted to a pure search for the numerical solutions of partial differential equation. The main idea of level set methods is to embed the propagating interface as the zero level set of a higher dimensional hyper-surface. By controlling the evolution of the hyper-surface, we can control the evolution of the curve. In literature, two general types of level set methods have been described: edge-based level set methods (Malladi et al., 1995), (Zhu et al., 2007), (Li et al., 2005), (Vasilevskiy and Siddiqi, 2002) and region-based level set methods (Chan and Vese, 2001), (Shi and Karl, 2008), (Li et al., 2008), (Lankton and Tannenbaum, 2008). The edge-based geodesic model is based on the relation between active contours and the computation of geodesics or minimal distance curves. This geodesic approach for object segmentation allows connecting classical “snakes” based on energy minimization and geometric active contours. However, main drawback of boundary-based level set segmentation methods is related to contour leakage at locations having weak or missing boundary data information. Specifically, these methods rely on the gradient-based edge function to stop curve evolution, and these models can detect only objects with edges defined by the gradients. In practice, discrete gradients are bounded;

stopping function is never zero on the edges. This allows the curve to pass through the boundary. One approach can be adopted to cope with these limitations: the region-based active contour. The region-based active contour method is a different kind of active contour model without a stopping edge-function, i.e., a model not employing gradient of the image for the stopping process. In this work, we present a semi-automatic segmentation approach for images with multiple objects based on the region-based level set technique, due to their recovery ability of objects with unknown topologies. This paper makes the following contributions;

- Analysis of Chan-Vese Model for image segmentation
- Develop a generalized CV model by incorporating local information in energy functional for segmentation of multiple object images.

Remaining paper is organized as follows; Section 2 describes a brief review of related work. We present our proposed method to overcome the limitations of previous works in section 3. In section 4, we provide experimental results. Finally, conclusions are given in section 5.

## 2. Related Work

### 2.1. Mumford-Shah (MS) Model

Mumford and Shah (1989) firstly proposed a general image segmentation model for 2D images. Using this model, the image is decomposed into some regions. Inside each region, the original image is approximated by a smooth function. Optimal partition of the image can be found by minimizing the Mumford-Shah (MS) functional. In addition, the model has a level set formulation, interior contours are automatically detected, and the initial curve can be anywhere within the image.

Let  $\Omega \in \mathbb{R}^N$  be a bound domain with Lipschitz boundary, modeling the image domain. Let  $u_0: \Omega \rightarrow \mathbb{R}$  represent a grayscale image. To find the segmentation  $C_0$  of  $u_0$ , Mumford-Shah (1989) has defined piecewise smooth segmentation function to carry out the following minimization:

$$E^{MS}(u, C) = \int_{\Omega} (u_0(x, y) - u(x, y))^2 dx dy + \mu \int_{\Omega \setminus C} |\nabla u(x, y)|^2 dx dy + \nu |C| \quad (1)$$

where  $u$  is a nearly piecewise smooth approximation of  $u_0$ ,  $\mu$  and  $\nu$  are positive constants, and  $C \subset \Omega$  denotes the smooth and closed segmenting curve.

Chan-Vese (2001) has modified the MS

model by considering a level set approach to solve the MS functional.

### 2.2. Chan-Vese (CV) Model

The CV model is an alternative solution to the MS segmentation problem which solves the minimization of (1) by using the level set method. As a starting point, we assume that the image  $u_0$  has two regions with piecewise-constant intensities, distinct values  $u_0^1$  and  $u_0^0$ . Further, assume that the object to be detected is represented by the region with the value  $u_0^1$ . Denote its boundary by  $C_0$ . Then we have  $u_0 \approx u_0^1$  inside( $C_0$ ) and  $u_0 \approx u_0^0$  outside( $C_0$ ). The global fitting term is defined as:

$$E_1(c_1, C) + E_2(c_2, C) = \int_{inside(C)} |u_0(x, y) - c_1|^2 dx dy + \int_{outside(C)} |u_0(x, y) - c_2|^2 dx dy \quad (2)$$

where,  $C$  is any other variable curve, constants  $c_1, c_2$  are  $C$  dependent and represent the averages of  $u_0$  inside  $C$  and outside  $C$  respectively.

In order to solve more complicated segmentation problem, we require regularizing terms, like the length of the curve  $C$ , or the area of the region inside  $C$ . The CV energy functional  $E^{CV}(c_1, c_2, C)$  is defined as

$$E^{CV}(c_1, c_2, C) = \mu \cdot Length(C) + \nu \cdot Area(inside(C)) + \lambda_1 \int_{inside(C)} |u_0(x, y) - c_1|^2 dx dy + \lambda_2 \int_{outside(C)} |u_0(x, y) - c_2|^2 dx dy \quad (3)$$

where  $\mu$ ,  $\lambda_1$ ,  $\lambda_2$  are positive constants, usually fixing  $\lambda_1 = \lambda_2 = 1$ , and  $\nu = 0$ .

This makes it suitable for images with weak edges and regions of piecewise constant intensities, which fits the characteristics of some images. However, main limitation of this model is that some objects cannot be detected using only the mean values of image intensities inside and outside curve  $C$ . In multiple region segmentation problems, the images usually have multi-objects with their intensity variations surrounding the background. By using the CV model, some objects of the foreground are incorrectly identified as the background. More specifically, if the mean value of the region inside  $C$  has a greater intensity than that of the region

outside  $C$ , objects that have low-intensities in the foreground cannot be segmented. Similarly, if the mean value of the region inside  $C$  has a lesser intensity than that of the region outside  $C$ , objects that have high-intensities in the foreground cannot be detected. Moreover, with different initial curves, different mean values of the regions inside and outside  $C$  can lead to poor or incorrect segmentation.

### 3. The Proposed Model

Keeping in view of the above mentioned limitations of CV model, we develop an improved image segmentation technique based on level set method by integrating local information. In this context, we propose a new energy functional in CV model and label as "Generalized Chan-Vese model" which is defined by

$$\begin{aligned}
 E(c_1, c_2, c_1^{max}, c_1^{min}, \Phi) &= \mu. Length(C) + v. Area(inside(C)) \\
 &+ E_L(c_1^{max}, c_1^{min}, c_2, \Phi)H(c_1^{max} - c_2)H(c_2 - c_1^{min}) \\
 &+ E_G(c_1, c_2, \Phi)[1 - H(c_1^{max} - c_2)H(c_2 - c_1^{min})]
 \end{aligned}
 \tag{4}$$

where  $H$  is a Heaviside function,  $\Phi$  is a level set function, the constants  $c_1^{max}, c_1^{min}$  depending on  $C$  and are the averages of high-intensity regions and low-intensity regions inside  $C$ , respectively.

Note that regularizing terms are determined in a similar fashion as described in Chan-Vese model (2001).

$$Length(C) = \int_{\Omega} \delta(\Phi(x, y)) |\nabla \Phi(x, y)| dx dy \tag{5}$$

$$Area(inside(C)) = \int_{\Omega} H(\Phi(x, y)) dx dy \tag{6}$$

And, the local and global fitting terms are calculated by using expressions given in eq. (7) and (8), respectively.

$$\begin{aligned}
 E_L(c_1^{max}, c_1^{min}, c_2, \Phi) &= \lambda_1 \int_{\Omega} |u_0(x, y) - c_1^{max}|^2 T(x, y) H(\Phi(x, y)) dx dy \\
 &+ \lambda_2 \int_{\Omega} |u_0(x, y) - c_2|^2 (1 - H(\Phi(x, y))) dx dy \\
 &+ \lambda_3 \int_{\Omega} |u_0(x, y) - c_1^{min}|^2 [1 - T(x, y)] H(\Phi(x, y)) dx dy
 \end{aligned}
 \tag{7}$$

$$\begin{aligned}
 E_G(c_1, c_2, \Phi) &= \lambda_1 \int_{\Omega} |u_0(x, y) - c_1|^2 H(\Phi(x, y)) dx dy \\
 &+ \lambda_2 \int_{\Omega} |u_0(x, y) - c_2|^2 (1 - H(\Phi(x, y))) dx dy
 \end{aligned}
 \tag{8}$$

where  $T(x, y)$  is a decision function of considered point  $(x, y)$ , which is used to decide whether  $(x, y)$  belongs to the high-intensity region or the low-intensity region. In this work, the decision function  $T(x, y)$  is given by (9).

$$T(x, y) = H(u_0(x, y) - c_2) \tag{9}$$

Then, fitting image  $u$  can simply be written using the level set formulation as

$$\begin{aligned}
 u(x, y) &= u_L(x, y)H(c_1^{max} - c_2)H(c_2 - c_1^{min}) \\
 &+ u_G(x, y)[1 - H(c_1^{max} - c_2)H(c_2 - c_1^{min})]
 \end{aligned}
 \tag{10}$$

$$\begin{aligned}
 \text{with} \\
 u_L(x, y) &= (c_1^{max}T(x, y) + c_1^{min}[1 - T(x, y)])H(\Phi(x, y)) \\
 &+ c_2(1 - H(\Phi(x, y)))
 \end{aligned}
 \tag{11}$$

$$\begin{aligned}
 u_G(x, y) &= c_1H(\Phi(x, y)) + c_2(1 - H(\Phi(x, y)))
 \end{aligned}
 \tag{12}$$

Keeping  $\Phi$  fixed and minimizing the energy function  $E(c_1, c_2, c_1^{max}, c_1^{min}, \Phi)$  with respect to the constants  $c_1$  and  $c_2$  in  $E_G(c_1, c_2, \Phi)$  and  $c_1^{max}, c_1^{min}$  and  $c_2$  in  $E_L(c_1^{max}, c_1^{min}, c_2, \Phi)$ .

For global energy function, two constants  $c_1$  and  $c_2$  are determined using eq. (13) and (14), respectively as given in Chan-Vese model (2001).

$$c_1(\Phi) = \frac{\int_{\Omega} u_0(x, y)H(\Phi(x, y)) dx dy}{\int_{\Omega} H(\Phi(x, y)) dx dy} \tag{13}$$

$$c_2(\Phi) = \frac{\int_{\Omega} u_0(x, y)(1 - H(\Phi(x, y))) dx dy}{\int_{\Omega} (1 - H(\Phi(x, y))) dx dy} \tag{14}$$

For local energy function, its constants  $c_1^{max}, c_1^{min}$  are defined by:

$$c_1^{max}(\Phi) = \frac{\int_{\Omega} u_0(x, y)T(x, y)H(\Phi(x, y)) dx dy}{\int_{\Omega} T(x, y)H(\Phi(x, y)) dx dy} \tag{15}$$

$$c_1^{min}(\Phi) = \frac{\int_{\Omega} u_0(x, y)(1 - T(x, y))H(\Phi(x, y)) dx dy}{\int_{\Omega} (1 - T(x, y))H(\Phi(x, y)) dx dy} \tag{16}$$

Finally, keeping these constants fixed, and minimizing  $E$  with respect to  $\Phi$ :

$$\frac{\partial \Phi}{\partial t} = \delta(\Phi) \left[ F_G \cdot H(c_1^{max} - c_2) H(c_2 - c_1^{min}) + \right. \\ \left. FL \cdot 1 - Hc1max - c2Hc2 - c1min \right] \quad (17)$$

with

$$F_G = \mu \operatorname{div} \left( \frac{\nabla \Phi}{|\nabla \Phi|} \right) - v - \lambda_1 (u_0 - c_1)^2 \\ + \lambda_2 (u_0 - c_2)^2 \quad (18)$$

$$F_L = \mu \operatorname{div} \left( \frac{\nabla \phi}{|\nabla \phi|} \right) - v - \lambda_1 (u_0 - c_1^{max})^2 H(u_0 - c_2) \\ + \lambda_2 (u_0 - c_2)^2 - \lambda_3 (u_0 - c_1^{min})^2 [1 - H(u_0 - c_2)] \quad (19)$$

Our experimental study shows that the accuracy of the proposed method is significantly improved as compared with the original Chan-Vese model (2001) for multiple object segmentation of 2D images.

#### 4. Experimental Results

In this section we present simulation results, obtained through the proposed approach Generalized Chan-Vese model, for 2D images. All experiments are performed in Matlab 7.8.0 (R2009a) with an AMD Phenom 9600 Quad-Core 2.30 GHz machine. Further, user sets the initial fronts during initialization stage.

##### 4.1. Multiple Objects Segmentation

In the section, we examine the performance of the proposed approach for 2D image examples. Further, we show the robustness of the proposed method against artifacts and noise considering as multiple object segmentation problems. In first example, the input images are depicted in Fig. 1(a) and 1(d), which show multiple objects embedded in noisy environments. Fig. 1(b) and 1(e) show the initial curves are set by the user. Finally, results obtained through the proposed method are shown in Fig. 1(c) and 1(f). From visual results depicted in Fig. 1, it may be observe that the method achieved the desired target i.e. the proposed method is able to obtain two contours close to the objects' boundaries.

In addition to this, the proposed algorithm is applied to the sample image shown in Fig. 2(a), which consists of three connected components having greater or lesser intensities than that of the background. The same initialization is used as was set in Fig. 1(e), which is depicted by the red curve in Fig. 2(b). From the Fig. 2(c), we can see that the method is able to obtain object boundaries regardless of object brightness.

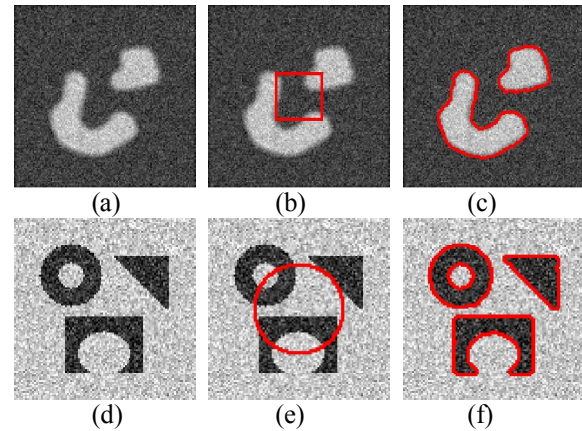


Figure 1. Multiple objects segmentation in noisy environment. (a), (d) Original image. (b), (e) Initial curve. (c), (f) Final results obtained with proposed method.

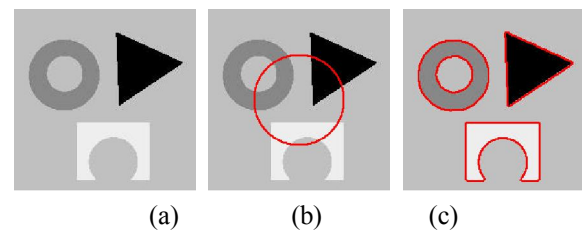


Figure 2. Segmentation result of multiple objects image. (a) Original image, (b) Initial curve, (c) Final result of proposed method.

##### 4.2. Comparison of the Proposed Approach with State of the Art Techniques

The following examples show the comparisons of our proposed model with other approaches. In this work, we compare our proposed approach with four well-known models: Caselles method (1997) (an edge-based level set method), Chan-Vese model (2001) and Shi method (2008) (global region-based level set techniques), and Li method (2008) (local region-based active contours approach).

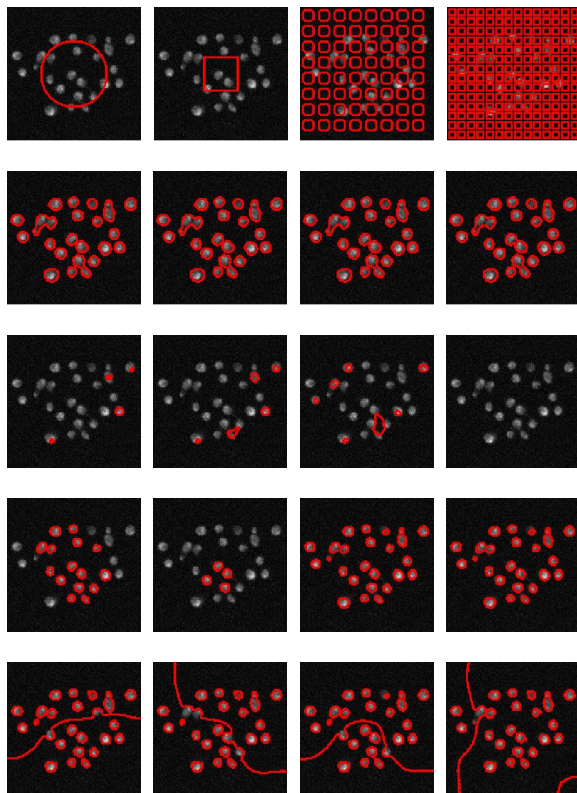


Figure 3. Segmentation of a fluorescence micrograph of yeast cells with different initializations. Each column corresponds to a given initialization. Top row: original images with the level set initialization. Second row: segmentation results using the proposed method. Third row: Segmentation results using a Caselles method (1997). Fourth row: Segmentation results using Chan-Vese model (2001). Last row: Segmentation results using Li method (2008).

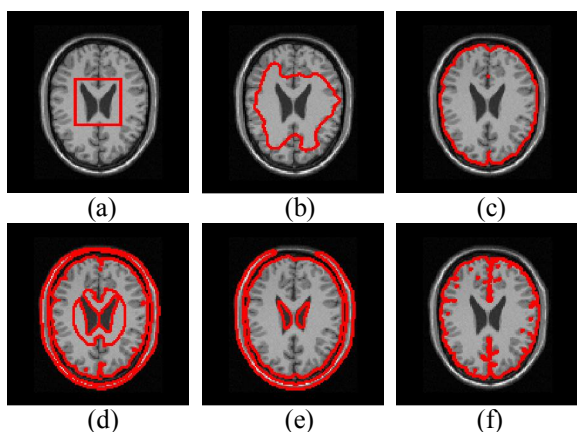


Figure 4. Segmentation results of brain MRI image. (a) Original image and its initial curve, (b) Caselles method, (c) Chan-Vese model, (d) Li method, (e) Proposed method, (f) Shi method.

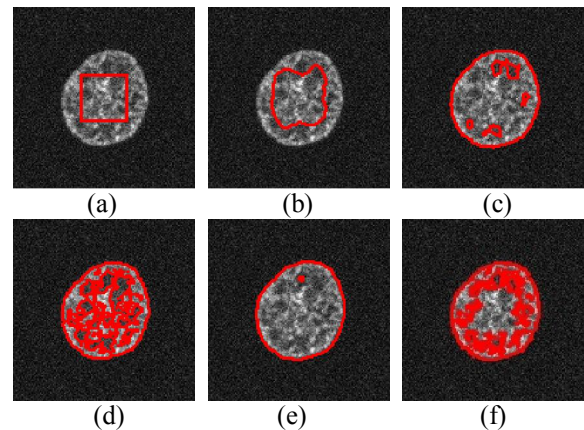


Figure 5. Segmentation results of brain Nucleus Fluorescence Micrograph image. (a) Original image and its initial curve, (b) Caselles method, (c) Chan-Vese model, (d) Li method, (e) Proposed method, (f) Shi method.

These segmentation approaches are qualitatively compared in the aspects of sensitivity to the location of initial contours and the accuracy of sub-pixel segmentation. Fig. 3 shows the segmentation results on a fluorescence micrograph – that contains labeled yeast cells – with different initializations. From Fig. 3, it can be observe that our proposed method is significantly less sensitive to noise and has better performance for images with weak edges or without edges.

To explore and present more comparison of the proposed approach with other related techniques, we have also considered many other examples including medical images and have carried out experimental analysis. Fig. 4 and Fig. 5 show the segmentation results of a brain MRI image and Water Country image, respectively. As we can observe from Fig. 4 and Fig. 5, the segmentation results of our proposed approach obtain the best performance compared with other methods.

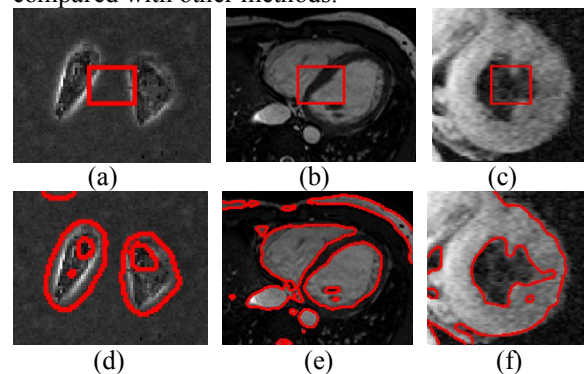


Figure 6. Medical images. (a) Two Cells Microscopy segmentation result, (b) Segmentation result of heart MRI image, (c) 2D MR image of the heart left ventricle segmentation result.

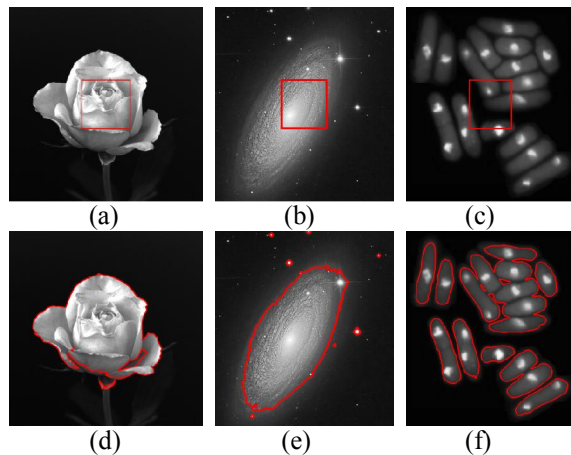


Figure 7. Real images segmentation. (a), (b) and (c) real images with their initial curves, (d), (e) and (f) segmentation results using the proposed approach.

In addition to this, obtained segmentation results on another medical and real image are shown in Fig. 6 and Fig. 7. Segmentation results shown in Fig. 6 demonstrate the usefulness of the proposed method in medical image segmentation applications. The first column of Fig. 6 shows a two cell microscopy image, the second column shows a heart MRI image and the last column shows a magnetic resonance image of the left ventricle of a human heart. As we can see from the experiment, the desired segmentation results can be obtained (the second row in Fig. 6).

Fig. 7 shows the segmentation results of real images by our proposed method (i.e., an image exhibiting saturation and noise, a galaxy image). The first row shows the initial contours which contain some parts of the objects. The second row shows the segmentation results using the proposed approach. We can see that the contours outlining the objects are accurately detected by our approach.

## 5. Conclusions

In this paper we have proposed a new region-based deformable model for image segmentation by integrating local information into the Chan-Vese model in order to overcome some limitations of this model. Performance comparison of the proposed technique with the well-known methods such as Caselles method, Chan-Vese model, Li method, Shi method shows that the proposed approach Generalized Chan-Vese model significantly improves the image segmentation results. Further, experimental results on real images also confirm its suitability for real image based applications.

## Acknowledgment:

This research was supported by Basic Science Research Program through the National Research Foundation of Korea (NRF) funded by the Ministry of Education, Science and Technology (No. 2011-0012586).

## Corresponding Author:

Professor, Jin Young Kim  
School of Electronics & Computer Engineering,  
Chonnam National University,  
Gwangju, South Korea  
E-mail: [beyondi@jnu.ac.kr](mailto:beyondi@jnu.ac.kr)

## References

1. M. Kass, A. Witkin, and D. Terzopoulos, Snakes: active contour models, *Int'l J. Comp. Vis.*, vol.1, no.4, pp. 321–331, 1987.
2. Black A, and Yuille A., *Active vision* (Cambridge: MIT Press, eds. 1993).
3. A. A. Amini, T. E. Weymouth, and R. C. Jain, Using dynamic programming for solving variational problems in vision, *IEEE Trans. Patt. Anal. Mach. Intell.*, vol.12, no.9, pp. 855–867, 1990.
4. L. D. Cohen, On active contour models and balloons, *CVGIP: Imag. Under.*, vol.53, no.2, pp. 211–218, 1991.
5. T. McInerney and D. Terzopoulos, A dynamic finite element surface model for segmentation and tracking in multidimensional medical images with application to cardiac 4D image analysis, *Comp. Med. Imag. Graph.*, vol.19, no.1, pp. 69–83, 1995.
6. V. Caselles, F. Catta, T. Coll, and F. Dibos, A geometric model for active contours, *Numerische Mathematik*, vol.66, pp. 1–31, 1993.
7. R. Malladi, J. A. Sethian, and B. C. Vemuri, Shape modeling with front propagation: a level set approach, *IEEE Trans. Patt. Anal. Mach. Intell.*, vol.17, no.2, pp. 158–175, 1995.
8. V. Caselles, R. Kimmel, and G. Sapiro, Geodesic active contours, *Int. J. of Computer Vision*, vol.22, pp.61-79, 1997.
9. R. T. Whitaker, Volumetric deformable models: active blobs, Tech. Rep. ECRC-94- 25, European Computer-Industry Research Centre GmbH, 1994.
10. G. Sapiro and A. Tannenbaum, Affine invariant scale-space, *Int'l J. Comp. Vis.*, vol.11, no.1, pp. 25–44, 1993.
11. B. B. Kimia, A. R. Tannenbaum, and S. W. Zucker, Shapes, shocks, and deformations I: the components of two-dimensional shape and the reaction-diffusion space, *Int'l J. Comp. Vis.*, vol.15, pp. 189–224, 1995.

12. R. Kimmel, A. Amir, and A. M. Bruckstein, Finding shortest paths on surfaces using level sets propagation, *IEEE Trans. Patt. Anal. Mach. Intell.*, vol.17, no.6, pp. 635–640, 1995.
13. L. Alvarez, F. Guichard, P. L. Lions, and J. M. Morel, Axioms and fundamental equations of image processing, *Archive for Rational Mechanics and Analysis*, vol.123, no.3, pp. 199–257, 1993.
14. S. Osher and J. A. Sethian, Fronts propagating with curvature-dependent speed: algorithms based on Hamilton-Jacobi formulations, *J. Computational Physics*, vol.79, pp. 12–49, 1988.
15. J. A. Sethian, *Level Set Methods and Fast Marching Methods: Evolving Interfaces in Computational Geometry, Fluid Mechanics, Computer Vision, and Material Science* (Cambridge, UK: Cambridge University Press, 2nd ed., 1999).
16. G. P. Zhu, Sh. Q. Zhang, Q. SH. Zeng, Ch. H. Wang, Boundary-based image segmentation using binary level set method, *SPIE OE Letters*, vol.46, no.5, 2007.
17. C. M. Li, C. Y. Xu, C. F. Gui, M. D. Fox, Level set evolution without re-initialization: a new variational formulation, *Proc. of IEEE Conference on Computer Vision and Pattern Recognition*, San Diego, pp. 430-436, 2005.
18. A. Vasilevskiy and K. Siddiqi, Flux-maximizing geometric flows, *IEEE Trans. Patt. Anal. Mach. Intell.*, vol.24, pp. 1565-1578, 2002.
19. T. Chan, L. Vese, Active contour without edges, *IEEE Trans. Image Process.*, vol.10, no.2, pp. 266-277, 2001.
20. Y. Shi and W. C. Karl, A real-time algorithm for the approximation of level-set based curve evolution, *IEEE Trans. Image Process.*, vol.17, no.5, pp. 645-656, 2008.
21. C. Li, C. Kao, J. Gore, and Z. Ding, Minimization of region-scalable fitting energy for image segmentation, *IEEE Trans. Image Process.*, vol.17, pp. 1940-1949, 2008.
22. S. Lankton and A. Tannenbaum, Localizing region-based active contours, *IEEE Trans. Image Process.*, vol.17, no.11, pp.2029-2039, 2008.
23. D. Mumford, and J. Shah, Optimal approximation by piecewise smooth function and associated variational problems, *Communication on Pure and Applied Mathematics*, vol.42, pp. 577–685, 1989.

02/05/2013